ANL-4982

Argonne National Laboratory

PHYSICS DIVISION
SUMMARY REPORT
JUNE through NOVEMBER 1952

ANL-4982
Physics

ARGONNE NATIONAL LABORATORY
P.O. Box 299
Lemont, Illinois

PHYSICS DIVISION

SUMMARY REPORT

JUNE through NOVEMBER 1952

Louis A. Turner, Division Director

MARCH 1953

Operated by The University of Chicago
under
Contract W-31-109-eng-38

TABLE OF CONTENTS

Report for June through November, 1952

Physics Division

TABLE OF CONTENTS CONTINUED

I. Cross Section for the Capture of Low Energy Neutrons by Protons
(B. Hamermesh, G. R. Ringo and S. Wexler)

The neutron-proton capture cross section has been found to be 0.329 ± 0.004 barns at 2200 meters per sec.

The method used, which was suggested by L. A. Turner, was to compare the hydrogen and boron capture cross sections by adding boron to a tank of water and measuring the effect this had on the capture, by the water, of neutrons from a constant source. This was detected by measuring the activity induced in NaI initially present in the water, first, in the solution without boron then, second, in the solution with boron.

$$R = \frac{\text{Activity of solution without boron}}{\text{Activity of solution with boron}} = \frac{N_{NaI}\,\sigma_{NaI}}{N_{NaI}\,\sigma_{NaI} + N_H\,\sigma_H} \Bigg/ \frac{N'_{NaI}\,\sigma_{NaI}}{N'_{NaI}\,\sigma_{NaI} + N'_H\,\sigma_H + N'_B\,\sigma_B}$$

Here the unprimed N's are the numbers of atoms per c.c. of the various materials in the solution without boron, the primed N's the same for the solution with boron; the σ's are the neutron absorption cross sections of the materials. (The capture in oxygen, < 0.2 mb, is neglected in writing this ratio.) The N's are obviously fairly easy to determine.

σ_{NaI} is easy to measure to about 3% and since N_{NaI} is so chosen that $N_{NaI}\,\sigma_{NaI} \approx 0.5\, N_H\,\sigma_H$ the error in σ_{NaI} is small in comparison with the other errors of this measurement. σ_B is determined by comparison of the boron used in this experiment with a standard boron whose absolute absorption cross section has been measured by transmission measurements.[1] The comparison is done by danger coefficient

[1] Kimball, Ringo, Robillard and Wexler, ANL-4680. P. 29, Sept. 1, 1951

measurements in CP-2. The point of the comparison is to take into account possible variations in the isotopic ratios in different samples of boric acid.

The solutions were activated by a beam from the thermal column of CP-3' led into a tank of water by means of a 2-5/8" ID Teflon tube, as shown in Figure 1. The strength of the boron was monitored by gold foils placed in the center of the 2" diameter opening in front of the tank. A correction was made for the effects of neutrons scattered back out of the hole or absorbed by the tube. It amounted to less than 0.2% in the value of R. The activities of the solutions were measured by thin-wall Geiger counters containing jackets for holding about 20 c.c. of liquid. Cadmium difference measurements were made and showed an epi-cadmium activation of about 7%.

The sources of error and their contributions to the error in σ_H are believed to be about as follows:

Standard deviation in values of R-1 (9 runs)	1.06%
σ of standard boron	0.4%
Comparison of borons	0.4%
Analysis of boron in solution	0.3%
Error in σ_{NaI}	0.2%
Error in N_H and N'_H (Actually errors in assumptions about densities of solutions)	0.1%

These combine to give a standard error of 1.26%.

In this measurement we obtain a ratio between the effective absorption cross sections of boron and hydrogen. Since boron is known to be a $1/v$ absorber in the thermal region to the accuracy of measurements

FIGURE 1.

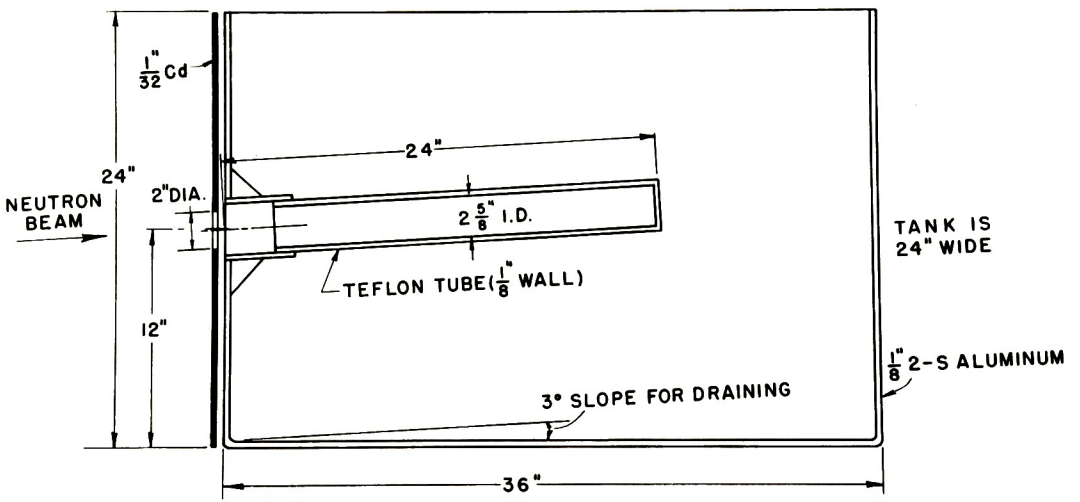

PHG-413
1-6-53
B.G.

made, and hydrogen is strongly expected to be one on theoretical grounds, the same ratio should apply for the cross sections at every energy in the thermal region. As a check, however, on possible spectral effects, a boron solution was irradiated at two temperatures 40° C. apart. The activities from the two irradiations, corrected for monitor variation, were found to be the same within the accuracy of the measurement - about 2%. This indicates that boron and hydrogen have about the same variation of absorption with energy as iodine - in all probability, $1/v$. In any event this shows that the difference in the spectrum in the solution with boron and the one without boron, which should be quite small, should not affect the division of the neutron captures between hydrogen, boron, and iodine.

The measurement could probably be pushed to an accuracy of 0.5% by using higher concentrations of boron and a larger number of runs, particularly if a higher flux pile such as CP-5 were available. We believe, however, this should wait until (1) it is clear such improved accuracy would be of sufficient importance for theory and (2) the σ of the standard boron is more certain.

II. A Survey of Total Cross Sections for 14-Mev Neutrons
(L. Goodman)

Neutrons produced by the T(D,n) He reaction were detected by observing pulses due to recoil protons in an anthracene crystal mounted on an RCA 5819 photomultiplier tube. The various absorbers were moved in and out of position by a remote crank-and-pulley system. The source could, therefore, be left on while the absorber was moved.

To avoid any possible error due to changing source or detector conditions, runs with "absorber in" and "absorber out" were alternated several times during a run, and appropriate averages were taken.

An anthracene crystal was chosen for a detector since it provides relatively high efficiency for a small size which makes geometrical corrections simple. For a proton of energy 12-14 Mev, the pulse in the crystal is about 60% of that for an electron of the same energy.[1] With the amplifier signal biased to discriminate against recoil protons of less than 12 Mev, discrimination is also achieved against electron pulses if the electron energy is less than 7.2 Mev. If an electron is more energetic than this, it still will not be counted since in the maximum distance that the electron can traverse in the crystal used, the electron can lose less than 7 Mev.[2] It is also improbable that an electron-positron pair would give up as much as 7 Mev in the crystal. Thus there is good discrimination against gamma-rays if any are produced by inelastic processes in the absorber, equipment, or walls.

---

[1] Taylor et al., Phys. Rev. 84, 1034 (1951).

[2] H. Bethe, Z. Physik 76, 298 (1932).

Regulation of the photomultiplier supply voltage was good enough to achieve about 1% regulation in pulse height for the worst line voltage fluctuation encountered (about 5%).

The detection of room-scattered neutrons was largely avoided by the above-mentioned biasing of the amplifier signal. Neutrons which were degraded in energy by scattering so that their energies were below 12 Mev could not be detected. The discriminator setting for the acceptance of the 12-14 Mev recoil protons was determined in the following manner. The source strength was measured by the activation of a copper foil (the 10 - min positron activity from the Cu^{63} $[n, 2n]$ Cu^{62} was counted with a G-M counter). From geometrical considerations, the amount of hydrogen in the anthracene crystal, and the known energy distribution of the recoil protons, the counting rate which would include only recoil protons in the energy group 12-14 Mev was calculated. The discriminator was then varied until this counting rate was obtained. This discrimination reduced the detection of room-scattered neutrons to 3% of the total number of neutrons detected with no absorber. This was measured by inserting an 11" long iron cylinder in the absorber position. The calculated transmission of this absorber is about 0.3%.

There are two effects which cause the apparent transmission to be larger than the true transmission. These are known as "room-scattering" and "in-scattering".

Room-scattered neutrons are neutrons which reach the detector by scattered paths other than in the cone subtended from the detector by the source. We call the number of neutrons counted which reached the detector via paths in this cone unity, and the number which were

room-scattered, the fraction "f".

If "T_a" is the apparent transmission, and "T" the true transmission, $T_a = (T + f)/(1 + f)$ or $T = T_a (1 - f(1 - T_a)/Ta)$. This correction was made for all measurements.

By "in-scattered neutrons" we mean neutrons which arrived at the absorber via a direct path from the source and were scattered into the detector. The in-scattering correction was carried out according to the procedure of McMillan and Sewell (MDDC-1558). Depending upon the size of the sample used, and the microscopic cross section of the material, this correction varied from 0.1% to 1%.

For hydrogen, the small correction for center of mass motion was included. This amounts to 0.8%. This effect was ignored for all other elements.

Since the cross sections of all the elements do not differ very much at this neutron energy, there is no necessity for extreme purity of the samples. All of the metal samples used were simply taken from stock or from special materials, machined to very close tolerance, and measured. The materials in stock are about 99% pure. In the case of nickel, the sample on hand was of doubtful origin, and a spectrographic analysis was, therefore, obtained from the Argonne Chemistry Division. The analysis showed about 3% cobalt, which was assumed to be unimportant.

The method of preparation of Be excludes significant impurities of heavy elements and allows a total maximum impurity of 1% distributed among Fe, Si, Mg, Al, and O.

The carbon sample was machined graphite of high purity. The hydrogen cross section was measured by subtraction, using polystyrene and subtracting off the carbon cross section. The deuterium cross section was measured by comparing equal molar amounts of H_2O and D_2O in the same machined container. A rough value of the oxygen cross section was determined incidentally in this measurement.

The cross section values with their standard deviations are given in the accompanying table. Errors due to other sources are negligible compared to the standard statistical counting errors and were, therefore, not included.

The figure is a plot of $\sigma^{1/2}$ vs. $A^{1/3}$ for the elements investigated. Elementary theory predicts a straight line relationship if $\lambda\!\!\!^{-} \ll R$ (which condition is not satisfied for all elements considered), and if the elastic cross section is equal to the inelastic cross section, which is also not the case for all elements. For these reasons, no attempt will be made here to evaluate nuclear radii in terms of the mass number "A" or to attach any other strong significance to the straight line drawn.

It might, however, be mentioned in passing that the points for H, D, Be, and Sb are all quite markedly off the line. This is not surprising at all for H and D since for these nuclei the effective nuclear radii are really the range of nuclear forces that would not be expected to fall on the $A^{1/3}$ line. Further, the inelastic cross section is certainly not equal to the elastic cross section for these isotopes.

For Be and Sb one might base speculation upon models in which there is a central core and a single particle outside.

FIGURE 2.

PLOT OF $\sigma^{\frac{1}{2}}$ vs $A^{\frac{1}{2}}$ FOR 14Mev NEUTRON CROSS SECTIONS

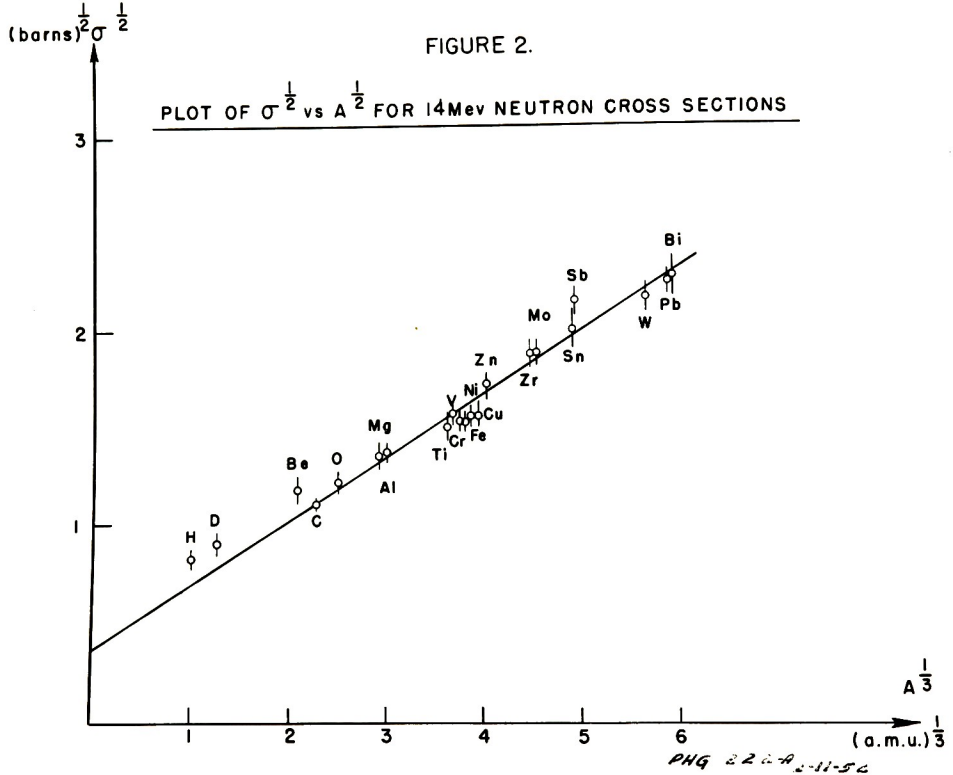

TOTAL CROSS SECTIONS FOR 14-Mev NEUTRONS

H	$0.69 \pm .06 \times 10^{-24}$ cm^2
D	$0.82 \pm .08$
Be	$1.4 \pm .1$
C	$1.20 \pm .04$
O	$1.5 \pm .1$
Mg	$1.8 \pm .2$
Al	$1.8 \pm .1$
Ti	$2.2 \pm .2$
V	$2.4 \pm .1$
Cr	$2.3 \pm .2$
Fe	$2.4 \pm .2$
Ni	$2.5 \pm .1$
Cu	$2.5 \pm .1$
Zn	$3.0 \pm .2$
Zr	$3.6 \pm .2$
Mo	$3.6 \pm .3$
Sn	$4.0 \pm .4$
Sb	$4.6 \pm .3$
W	$4.8 \pm .3$
Pb	$5.1 \pm .4$
Bi	$5.2 \pm .5$

The low value of 110 barns for the peak resonance cross section and the small initial bending of only 27% in the transmission curve both indicate that the scattering resonance in bismuth is not strong.

2. The Neutron Scattering Cross Sections of B, Sc, Hf, Pb and Bi

The average sub-cadmium and epi-cadmium scattering cross sections of several isotopes have been measured by use of the annular scattering counter. In the sub-cadmium energy region a standard foil made of vanadium powder of high purity attached to 1/2 mil aluminum foil by Zapon was used. Vanadium has no coherent scattering in this region, so that troublesome crystal effects were avoided. In the epi-cadmium region a thin foil of high purity graphite (machined) was used as a standard scattering detector. The cross sections of vanadium and graphite have previously been determined by self-detection, in which case no standard was required.

For B^{10} very thin foils were necessary to minimize absorption since this isotope has a large absorption cross section at low energies. Results obtained from the thinnest sample used are quoted herewith. The results for all isotopes measured are summarized in Table I.

Table I.
Scattering Cross Sections at Sub-Cadmium and Epi-Cadmium Neutron Energies

Element	Neutron Energy		Sample
	Sub-Cadmium	Epi-Cadmium	
B^{10}	2.4 barns	3.3 barns	Boron 96% enriched
Sc^{45}	23.4 "	16.6 "	Oxide
Hf	-----	34.2 "	Oxide
Hf^{177}	-----	52.5 "	Oxide 61.7% enriched
Hf^{178}	-----	43.1 "	Oxide 80.9% enriched
Pb	9.9 barns	10.8 barns	6 Mil foil
Bi	8.5 "	10.4 "	8 Mil foil

In the case of Sc^{45} Shull and Milligan[1] quote a coherent, thermal scattering amplitude of 1.02 (thermal coherent scattering 13.1 barns). This large value of the coherent along with a large total scattering cross section of 23.4 barns in the thermal region are possible only when a scattering resonance is present below thermal energy, presumably at some negative energy.

3. Neutron Transmission Cross Sections of B^{10}, Sc^{45} and Gd.

The total neutron cross sections of B^{10} (96% enriched), Sc^{45} and Gd (metal) have been measured at several neutron energies by use of the annular scattering counter and various detectors having large scattering resonances at known energies. These resonances scattering detectors serve to select neutrons at known energies. Detectors used are the following (along with the energy of the scattering resonance): V^{51} (for sub-cadmium and scattering resonances at 7 and 13 kev), Sm^{152} (8.2 ev), W^{186} (19.5 ev), Co (126 ev), Mn (principally at 345 ev), and Na (2800 ev).

A semi-logarithmic plot of the transmission for Sc^{45} usually resulted in a straight line. At some energies an initial bending occurred followed by an asymptotic straight part. This initial bending indicates the presence of a resonance in the absorber near the energy of the resonance in the detector foil. The percentage of initial bending, found by projecting the asymptotic part of the transmission curve back to zero thickness of absorber, is a measure of the proximity of the resonance in the absorber to that of the detector. By these means one

---

1 C. G. Shull, W. O. Milligan, Private Communications

or more resonances in Sc^{45} are indicated in the kev energy region.

Only one sample of Gd (metal) was available, but the unusually high cross sections indicate many resonances in the region covered. This has later been verified by the time-of-flight spectrometer group. Also resonances are indicated in the kev region for B^{10}.

The average epi-Cd total neutron cross section of Sc^{45} was determined (11.5 barns with 12% initial bending) by use of a carbon (graphite) detector, which has no resonance and detects as a "flat" detector. Further, a self-detection transmission curve for Sc^{45} using Sc_2O_3 as a detector indicated an asymptotic cross section of 17.6 barns with 21% initial bending.

The data of Shull and Milligan on coherent scattering of Sc^{45} and the data included in this report together point with considerable certainty to a resonance in the negative neutron energy region. An attempt to locate this resonance by use of the Breit-Wigner one-level formula produced inconsistent results. At present it can not be located any more accurately than to say that it probably lies between zero and minus 100 ev. The data reported here indicate that a two-or three-level Breit-Wigner formula must be used to take account of contributing resonances in the positive neutron energy region. Until the location of these resonances is known, further analysis is not possible. The analysis for B^{10} shows similar relationships.

Measured cross sections at the various energies are collected in Table II. Data reported at 8.2 ev have previously been reported, as at 10 ev. Recent measurements by Sailor et al[2] (B.N.L.) indicate that the resonance in Sm^{152} is at 8.20 rather than 10 ev.

2 V. L. Sailor, H. L. Foote, Jr., and H. H. Landon, Phys. Rev. 89, 904 (1953).

Table II - Total Neutron Sections

Element	Sample	Neutron Energy						
		Sub-Cd	8.2 ev	20 ev	126 ev	345 ev	2800 ev	V^{51} 7 and 13 kev
B^{10}	348.6 $\frac{mg}{cm^2}$	----	103 barns	73 barns	44 barns	21 barns	31 barns	24 barns
	11.4 $\frac{mg}{cm^2}$	1650 barns	----	----	----	----	----	----
	3.5 $\frac{mg}{cm^2}$	3180 barns	191 barns	91 barns	----	----	----	----
Sc^{45}	----	48.2 barns	21.6 barns	17.9 barns	14.8 barns	7.5 barns	10.4 barns 18% initial bending	12.7 barns 12% initial bending
Gd	5.032 $\frac{gm}{cm^2}$	----	30 barns	29 barns	26 barns	26 barns	27 barns	22 barns

4. Sub-Cadmium Absorption Cross Section of B^{10} and Sc^{45}.

From TableII of this report it may be seen that the apparent sub-cadmium cross section of B^{10} increases with decreasing thickness of the samples of B^{10}. Due to a large absorption cross section at low energy, the first thin layer is most effective in removing neutrons from the beam by absorption. Additional thickness of absorbing sample has a smaller effect on the beam. Ideally, then, the correct absorption cross section must be obtained from a sample of infinitesimal thickness. To approximate this the cross sections of the two thinnest samples measured were plotted against their thicknesses, and a line through these two points was extended to zero thickness. It was found to intercept the cross section axis at 3900 barns with an error of ± 400 barns due principally to uncertainties in samples. The previously accepted value of 3990 barns was determined by others from measurements made with ordinary boron, corrected for isotopic abundance. The present measurements were made on samples of B^{10}, 96% enriched.

Previous measurements of the cross section of Sc^{45} made by the pile oscillator method yielded a value of 31.8 b (A. N. L.) and 11.8 b (O. R. N. L.). This discrepancy prompted a measurement by use of the annular scattering counter. To obtain the absorption cross section it was necessary to measure both the total and scattering cross sections, the difference between them giving the absorption cross section.

From Table II of this report the total cross section is seen to be 48.2 barns for sub-Cd energy, and from Table I the scattering cross section is 23.4 barns. Thus, an absorption cross section of 24.8 barns results. Because of uncertainties concerning the sample and counting

statistics, the error in this value could be ± 2 barns.

H. Pomerance of Oak Ridge National Laboratory, in reply to a private communication, reports that a recent measurement of the thermal absorption cross section of Sc^{45} in that laboratory yielded a value of 23 ± 1.5 barns. A private communication to him from Littler and Lockett at Harwell, England, reported 24 barns, while an activation cross section by W. S. Lyon of Oak Ridge National Laboratory produced a cross section of 23 barns.

IV. Neutron Resonances in Gd and Cd
(R. Ronald Palmer)

The Argonne fast chopper has been used to measure the neutron transmission of gadolinium, cadmium, and the partially separated isotopes of cadmium. Most of these data have been taken at such a rotor speed that the neutron burst width is about 10 microseconds and with the detector system at a distance of 10 meters. Under these conditions the approximately triangular resolution function has a width at half-maximum of about 0.5 microseconds per meter. Data have been obtained for neutron energies down to about 1.0 ev.

Most of the data for gadolinium have been obtained using 1/4 inch thick gadolinium metal (5.04 gm per sq cm). Very deep transmission dips (essentially to zero) occur at 2.0 and 2.5 ev; a very prominent dip exists at 20.5 ev; fairly prominent dips exist at 6.2, 7.8, 11.6, 14.4, 16.5, 25, 33, 48, 79 and 108 ev; and there are others as yet less definitely located at higher energies. Cross section calculations will be made after further data have been obtained using a thinner sample.

The data for cadmium have been taken using 1-inch-thick cadmium metal (19.9 gm per sq cm). Very prominent resonances are observed at 27 and 85 ev; fairly prominent ones occur at 18, 65 and 380 ev. Still other less distinct resonances exist between the 85 and 380-ev resonances and also at higher energies. These should be more clearly resolved using a 20-meter flight path; the data for this are now being taken.

Small quantities of the partially separated isotopes of cadmium in the form of cadmium oxide have been examined over the resonance

region. The cadmium isotopes 108, 110, 111,112, 113, 114, and 116 were used, with a sample thickness of approximately 1 gm per sq cm in each case. The 27-ev resonance can definitely be assigned to Cd^{111}. A preliminary calculation gives it a level strength, $\sigma_0 \Gamma^2$, of about 40 barn-$(ev)^2$. The 85-ev resonance appears to be assignable to Cd^{110}, though this is as yet less certain.

V. Neutron Resonances in Isotopes of Mo.
(S. P. Harris)

The separated isotopes Mo^{92}, Mo^{95}, Mo^{96}, Mo^{97}, and Mo^{98} have been run in the neutron velocity selector. (For results with unseparated Mo see AECU-2040 and ANL-4659.) The following isotopic assignments have been made for Mo resonances:

Resonance Energy - ev	Isotope
44	Mo^{95}
70	Mo^{97}
130	Mo^{96}

There are indications of resonances at about 900 ev and 5000 ev in the Mo^{97} curve. All of the above isotopes were run in the form of the oxide MoO_3. Mo^{100} will be run in the near future, but the one remaining stable isotope, Mo^{94}, is not yet available in sufficient quantity.

VI. Velocity Selector Equipment
(L. M. Bollinger and R. R. Palmer)

Automatic Control Circuit

The automatic controls that have been applied to the Argonne fast chopper have been described in a previous report (ANL-4798). The controls that were designed to protect the rotor have worked well, but those designed to protect the accumulated data have been unreliable. The latter controls have therefore been modified, and now perform satisfactorily. These new controls attempt to protect the data by stopping the run if the rotor is stopped, or if the 100-channel analyzer fails; the run is interrupted if the total detector counting rate becomes too great, or the pile power falls below some pre-assigned limit.

Photo Cell Unit

Each cycle of the 100-channel time analyzer used with the chopper is initiated just as the chopper slits are approaching the open position. This rotor position is established by a light beam that is reflected from a mirror mounted on the rotor and sweeps across a slit viewed by a photomultiplier. The accuracy of the absolute energies measured with the chopper is dependent on the reliable operation of this photo cell unit.

A new photo cell system with greatly improved characteristics has been installed and is in use. The rise time of its light pulse is about 0.5 μ-sec for full speed operation. The systematic drift in the time of this pulse relative to the time at which the chopper slits are completely open has been less than 1 μ-sec in several months of operation, and no erratic behavior has been observed.

Sample Changer

Many cross sections measured with the Argonne fast chopper have been of limited absolute accuracy because of systematic drifts in the overall sensitivity of the detecting system of boron fluoride counters and associated circuits. The influence of this instability may be minimized by repeated alternation of open beam and sample runs, but to perform this operation manually is both time-consuming and tiresome for the operator. We have, therefore, constructed and put into operation equipment that automatically alternates the sample and open beam runs with a cycle time of 4 minutes. While the sample is in the beam the data are recorded on half of the time analyzer, and the other half is used to record the open beam data. The use of this apparatus should make possible the measurement of cross sections with high accuracy within energy ranges that contain no resonance structure.

An alternate use of the sample changer is to block the neutron beam periodically, during which time the background counting rate is automatically recorded. This second mode of operation has been successfully used for several weeks.

VII. The Liquid Scintillation Neutron Detector
(L. M. Bollinger and G. E. Thomas)

Muehlhause and Thomas (ANL-4798) have described a series of investigations of the fundamental properties of a liquid scintillation neutron detector. The liquid used in a detector of this kind is a mixture of a standard scintillating liquid and a boron-containing compound. A neutron, on entering this medium, is slowed down, then captured by the boron, which disintegrates into Li and an α-particle. These particles produce a scintillation flash that may be detected to give a "neutron" count. The present report is a description of an attempt to use such a liquid counter as the detecting system of the Argonne fast chopper.

The counter has the following properties: Its scintillating liquid consisted of 4 gm/l of terphenyl and 8 mg/l of diphenylhexatriene in a mixture of equal parts of phenylcyclohexane and tri-methyl borate. This liquid was contained in a quartz cylinder 2 inches in diameter and 4 inches long. The outside surface of the cylinder was coated with a reflector consisting of MgO bonded by clear Zapon. To each end of the cylinder was attached a 5819 photomultiplier. This counter and its associated electronic equipment was located in a wooden shed 25 meters from the chopper.

To eliminate counts from photomultiplier noise, the complete counter described above was cooled to about 0°C, and the two photomultiplier output pulses were independently amplified and placed in coincidence. It was found, for thermal neutrons, that the ratio of single to coincidence counting rate was 1.4. Also, the ratio of

the sum of the two single rates to the coincidence rate was 1.9. These ratios could not be decreased by increasing the gains of the two photomultiplier systems. It was concluded, therefore, that coincidences were lost because the quantity of light emitted in some scintillations was not large enough to assure the formation of at least one electron at each photomultiplier cathode.

The data obtained with the liquid scintillator in conjunction with the chopper consist of a series of runs giving counting rate as a function of time-of-flight for various operating conditions. The time-dependent part of the counting rate is composed of a large peak in the neighborhood of $\tau = 0$ followed by a rate that varies roughly as $1/\tau$, where τ is the time of flight. The initial peak is largely caused by γ-rays that pass thru the chopper slits while they are in the open position, and the $1/\tau$ variation in rate is caused by neutrons from the chopper. It should be noted that a $1/\tau$ variation is expected for neutrons having a 1/E energy distribution when they are detected by a counter having an efficiency independent of energy. The time-dependent counting rate is superposed on a large time-independent counting rate.

A crude estimate of the efficiency of the liquid counter was made by comparing its counting rates at 25 meters with the counting rate of a BF_3 gas counter of known efficiency at 20 meters from the chopper. The efficiency obtained from this somewhat indirect comparison is 30% for neutrons of 6-kev energy, when the counter is operated as a coincidence device. Note that this value implies an efficiency of 55% if the photomultiplier pulses are added rather than put into coincidence.

These values are to be compared with an efficiency of about 3% for a 12-inch-long BF_3 gas counter filled to 2 atmospheres pressure.

The major drawback to using the liquid neutron counter as a practical tool with the chopper is its large background counting rate. The γ-ray peak at zero time-of-flight constitutes a time-dependent background that is bothersome for times-of-flight less than about 3 times the burst width of the chopper, that is, for about 30 μ-sec. It has been found that the relative magnitude of this initial peak may be reduced to a satisfactory level by excluding large photomultiplier pulses. When the detector is operated in this way, for a 25-meter flight path the initial peak constitutes a background only for times-of-flight corresponding to energies greater than 10 kev.

The elimination of the time-independent background is a much more difficult problem. In an effort to reduce this background, the counter was completely encased in 1/4 inch of lead, and then surrounded by 3 to 4 inches of lead with a 2-1/2 by 5-inch opening to admit the neutron beam from the chopper. Cadmium surrounded some of this lead. The neutron beam was collimated to the detector opening by a 3-foot-long channel of concrete block. Ahead of the concrete block there was a 2-inch-thick lead wall. This shielding of the counter reduced the background rate from 150 to 10 counts/sec.

This steady background is about twice as great as the rate resulting from chopper neutrons with 1-kev energy. It becomes progressively less important at higher energies.

A series of tests on the 10 counts/sec that remain with the shielding in place showed that they may be attributed to the following sources:

A. 38% High energy neutrons through the chopper rotor.

B. 17% Pile γ-rays into shielding collimator.

C. 15% Pile neutrons through shielding.

D. 30% Local contamination and cosmic rays.

Pulse-height distributions were obtained for these several kinds of backgrounds in the hope that they could be reduced by pulse-height analysis. It was found that very little improvement can be obtained in this way.

It is expected, however, that all four types of background listed above can be further reduced. The effects of radiation from the pile, other than that through the rotor, can be entirely eliminated with sufficient shielding. Further, preliminary tests show that the background produced by neutrons passing through the rotor can be reduced by a factor of two by collimation of the neutron beam at the exit end of the chopper. No effort has been made to determine the nature of the background termed "local contamination", but it is well known that lead is not the best shielding for low background work. It seems safe to assume, therefore, that the background may be reduced to a level such that its rate will be less than the signal rate for neutrons of 1 kev. The liquid scintillator can be used as a practical neutron detector for transmission measurements when this goal is attained.

VIII. Neutron Capture Gamma-Ray Spectra

(Bernard Hamermesh and Virginia Hummel)

Summary of Results Obtained to Date

We have been using a NaI-Tl scintillator in conjunction with a 5819 photomultiplier as a gamma-ray spectrometer to study neutron capture gamma-ray spectra. Various results have been reported in previous quarterly reports over the past year and a half. We summarize these results here and add some not previously reported.

Table III. Prominent thermal neutron capture gamma-rays from the elements Z = 17-30

Element	Sample	Gamma-ray energy (Mev)
Cl	C_2Cl_6	0.784 ± 0.010 1.15 ± 0.010 1.59 ± 0.013 2.00 ± 0.025 6.2 ± 0.2, 7.7 ± 0.2
K	Fluoride	6.0, 8.2
Ca	Metal	6.8, 8.2
Sc	Oxide	0.152, 0.220, 7-9
Ti	Oxide	1.0, 1.38, 5.0, 6.5-7.0
V	Metal	5.3, 5.7, 6.8, 7.4
Cr	Metal	0.880, 5-6, 8.0-8.5, 8.5-9
Mn	Metal	0.090, 0.190, 5.0, 7.2
Fe	Metal	0.425, 6.0, 7.4, 8.5
Co	Oxide	0.220, 1.1, 1.5, 5.8, 7.0
Ni	Metal	6.5-7.5, 8.5-9
Cu	Metal	0.150, 6.5-7, 7-8
Zn	Metal	1.0, 7.5

Table IV. Prominent thermal neutron capture gamma-rays from the elements Z = 45-57

Element	Sample	Gamma-ray energy (Mev)
Rh	Metal	0.080, 0.160
Pd	Metal	Unresolved
Ag	Metal	0.187
Cd	Metal	0.558, 8.5
In	Metal	0.160, 0.256
Sn	Metal	7.5-8.0
Sb	Metal	Unresolved
Te	Metal	0.609
I	CHI_3	Unresolved
Cs	Nitrate	Unresolved
Ba	Metal	Unresolved
La	Metal	4.5

Table V. Prominent thermal neutron capture gamma-rays from the elements Z = 72-83

Element	Sample	Gamma-ray energy (Mev)
Hf	Metal	Unresolved 0.220 line from Hf^{179} observed
Ta	Metal	Unresolved
W	Metal	5.0
Re	Metal	5.0
Os	Metal	5.0
Ir	Metal	5.0
Pt	Metal	5.0
Au	Metal	0.070, 6.2 and 0.411 from β decay
Hg	Oxide	0.335, 1.22, 4.85, 5.93
Tl	Metal	Unresolved
Pb	Metal	7.5
Bi	Metal	Unresolved

The First Four Excited States of Cl^{36}

The results given in the tables show no systematic structure of the spectra. In the case of chlorine, however, interesting conclusions can be drawn since the spectrum has recently been studied with the pair spectrometer by Kinsey, Bartholemew, and Walker.[1] The decay scheme of Cl^{36} that is presented in Figure 10 of their paper proposes that the first four excited states have the energies 0.79 ± 0.04, 1.14 ± 0.04, 1.58 ± 0.04 and 1.94 ± 0.07 Mev respectively. These energies are

[1] B. B. Kinsey, G. A. Bartholomew, and W. H. Walker, Phys. Rev. 85, 1012 (1952).

obtained by subtracting from the neutron binding energy of Cl^{36} the energies of the lines which Kinsey, et al., label B-E. The neutron binding energy has been reported as 8.54 Mev by Shrader and Pollard[2] and 8.49 Mev by Ennis.[3] Kinsey, et al., find that the most energetic gamma-ray from Cl^{36} has an energy of 8.56 ± 0.03 Mev. This line probably arises from a ground state transition from the initial state of Cl^{36} that is formed upon neutron capture.

The lines that we find at 0.784, 1.15, 1.59, and 2.00 Mev correspond to the transitions to the ground state from the levels reached by Kinsey's lines B-E in Cl^{36}. The line at 6.2 Mev is probably Kinsey's line F, and the line at 7.7 Mev is probably his line B. The 7.7-Mev line and the 0.784-Mev line are in cascade. The error in our measurement of the 7.7-Mev line does not permit us to make a good binding energy determination from our data alone.

If we label our four lowest lines B-E and combine each of them with Kinsey's line of the corresponding letter, then the following values for the neutron binding energy of Cl^{36} are found.

Neutron Binding Energy of Cl^{36} from Combined Scintillation Spectrometer and Pair Spectrometer Data

Line	Scintillation Spectrometer	Pair Spectrometer	Binding Energy of Cl^{36}
A	----	8.56 ± 0.03	8.56 ± 0.03
B	0.784 ± 0.010 Mev	7.77 ± 0.03 Mev	8.55 ± 0.03
C	1.15 ± 0.010	7.42 ± 0.03	8.57 ± 0.03
D	1.59 ± 0.013	6.98 ± 0.03	8.57 ± 0.03
E	2.00 ± 0.025	6.62 ± 0.06	8.62 ± 0.06
		Weighted average	8.57 ± 0.03

2 E. F. Shrader and E. Pollard, Phys. Rev. 59, 277 (1941).
3 W. W. Ennis, Phys. Rev. 82, 304 (1951).

The results in the table indicate that these four branches of the capture gamma decay scheme of Cl^{36} involve only two steps. Of course, the order of emission of the two lines in a branch is not definitely known. However, on the basis of our present knowledge (dependence of intensity on energy difference), it seems more likely that the more energetic transition in a given branch will occur first. This would mean that the four lowest lines that we observe arise from the first four excited states of Cl^{36}.

IX. Radiations of Rh^{104m} and Rh^{104}

(W. C. Jordan)

Neutron irradiation of rhodium produces two activities, a 4.3-minute isomeric transition and a 44-second beta decay to palladium. Conversion electron groups have been reported to be associated with the 4.3-minute activity by several investigators with considerable variation in the number of groups and energy values observed.[1] Gamma transitions of ~50 and 80 kev have been reported[2], and an energy of 52 kev is quoted from a scintillation spectrometer measurement.[3]

A spectrometer measurement of the 44-second beta transition results in an energy of 2.6 Mev.[4] Gamma transitions of 41, 180, and 950 kev have been reported[5] by absorption measurements to be associated with this period while one investigator[6] concludes that most of the electromagnetic radiation is bremsstrahlung. Gamma-rays of 560 kev and 1.1 Mev have been observed with a scintillation spectrometer.[7]

In the present investigation 180° photographic spectrometers are used to detect the conversion electrons. These are equipped with fast-operating vacuum locks to permit the rapid insertion of sources. The spectrometers and their operation are essentially the same as that described by Rutledge, Cork and Burson.[8] No-screen x-ray emulsions on both film and plate backings were used. All energy and density measurements were made with plates. The electron spectrum was searched from

---

1 Nuclear Data, NBS Circular 499.

2 M. Ageno, Nuovo Cimento 1, 415 (1943).

3 E. der Mateosian, M. Goldhaber, Phys. Rev. 82, 115 (1951).

4 N. Hole, Arkiv Mat., Astron, Fysik 34B, No. 5 (1947).

5 P. Chudom, C. O. Muehlhause, Plutonium Project Report CP-3801, p. 25 (1947).

6 B. N. Cacciapuoti, Nuovo Cimento 4, 31 (1947).

7 D. Maeder, P. P. Preiswerk, Helv. Phys. Acta 24, 625 (1951).

8 W. C. Rutledge, J. M. Cork, S. B. Burson, ANL-4735.

9 kev to ~2.5 Mev in three overlapping sections by using fields of 119.5, 442, and 812 gauss.

Five low energy conversion lines were observed to be associated with the 4.3-minute period. Their energy and interpretation is summarized in the following table.

Electron Energy (kev)	Corrected Intensity	Interpretation	Energy Sums (kev)	Gamma Energy (kev)	K/L	Type of Transition
27.9	13.5	K (Rh)	51.1			
				51.1	~5	M1 or M2
47.8	~2.9	L_1 (Rh)	51.2			
54.0	62	K (Rh)	77.2			
74.1	100	L_2 (Rh)	77.2	77.2	0.62 ± 0.15	E3
76.1	7.8	M (Rh)	77.2			

The area under the peak of a densitometer trace is taken as a measure of the intensity of a line. These measurements are corrected for geometrical attenuation by normalizing to a constant radius. The correction, for energy sensitivity of the emulsion used, was determined by Cork.[9] The total corrections are less than 15% for all of the lines except the 27.9-kev line. In this case it is 75%.

In addition to the study of conversion electrons an examination has been made with NaI (Tl) scintillation spectrometers, made available for this research by B. Hamermesh and V. Hummel. This equip-

---

[9] J. M. Cork (Private Communication).

ment consists of two spectrometers which can be operated independently or in coincidence. One is equipped with a twenty-channel analyzer, the other with a single-channel analyzer.

There are three prominent peaks in the pulse-height distribution of neutron-activated rhodium. They are due to 20, 51, and 550-kev transitions. The 20-kev is undoubtedly the Rh K x-ray. An additional small peak is observed corresponding to a transition of $\sim$1.2 Mev. A peak corresponding to the 77-kev transition is very small compared to the 51-kev peak. The x-ray and 51-kev peaks decay with only the 4.3-minute half life while the 550-peak exhibits both periods.

A systematic search was made for coincidences by setting the single-channel spectrometer at each of the three prominent peaks and scanning the coincidence spectrum with the twenty-channel spectrometer. Transitions observed to be in coincidence were x-ray - x-ray and x-ray - 51 kev. This is what one would expect if the 51-kev and highly converted 77-kev transitions are in cascade. No gamma-gamma or gamma-x-ray coincidences were observed with the single channel set at the 550-kev peak. There is, however, some evidence of beta-gamma coincidences in the case of the 550-kev transition.

Beryllium filters of $\sim 1.8 \frac{\text{gm}}{\text{cm}^2}$ were used to shield the detectors from the direct beta radiation. In the case of beta-gamma measurements the filter was used on only the twenty-channel side. The standard formula for calculation of accidental coincidence ratio is used. The accidental rate in the j'th channel of the twenty-channel analyzer is given by

$$Aj = 2T\, NNj$$

where N is the single counting rate on the single channel side and Nj is the single counting rate in the j'th channel of the twenty-channel side. The resolving time T was determined to be 7.5×10^{-6} seconds.

It should be noted that the above formula is not correct for a decaying source.[8] However, the more cumbersome formula for a decaying source introduces only a small correction for counting intervals less than two half-lives. A more serious error lies in the determination of Nj since it is not recorded during a coincidence count. This was determined from a short (1-minute) normal count before each coincidence count. The counting rate in the j'th channel was then assumed to decay in the same manner as the counting rates in the single-channel side which are recorded during both normal and coincidence counting. Since the 44-sec activity was allowed to come to equilibrium with the 4.3-min before counting was started, this is probably a reasonable assumption. Certainly the "peak" channel will be decaying at the same rate. For "valley" channels this leads to too low a value for Nj.

The coincidence data show that the 51 and 77-kev transitions are in cascade and indicate that the 550-kev transition follows the beta decay.

From a comparison of the observed K/L ratios and empirical K/L versus Z^2/E relations[10] one could assign a multipolarity M1 or M2 to the 51-kev transition and E3, E4, or M4 to the 77-kev transition. Accepting these possibilities one finds from lifetime-energy considerations that the 77-kev transition is the 4.3-min one and must be E3. The half-life of the 51-kev transition would be $\sim 10^{-10}$ sec for M1 and $\sim 10^{-3}$ sec for M2.

10 M. Goldhaber, A. W. Sunyar, Phys. Rev. 83, 906 (1951).

The beta transition was measured only by a crude absorption technique. The result was in agreement with other reported energy values.[1] The log (ft) value of 4.7 indicates a spin change of one and no change in parity.

Tentative decay scheme.

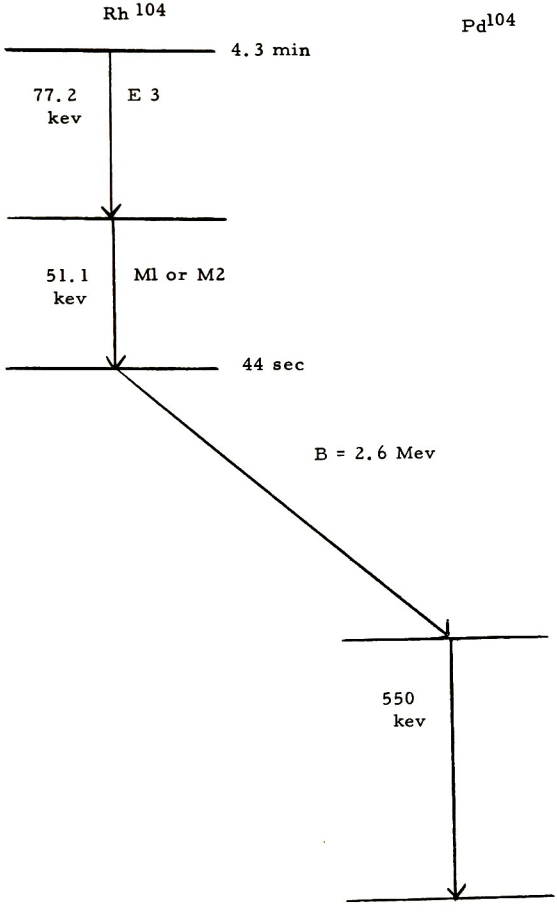

X. The Energy of Sb-Be Photo-neutrons
(Richard J. Culp)

Gamma radiation from Sb^{124} falling upon beryllium causes the photo emission of neutrons. The threshold for photo emission in beryllium is approximately 1.63 Mev, and the energy of the single gamma quantum from Sb^{124} is approximately 1.67 Mev. The combination of these two elements provides a copious source of nearly monoenergetic neutrons, and has been used extensively for activation cross section measurements. The uncertainty in the energy of these neutrons(circa 30 kev) is small enough to make competition with variable energy particle accelerators feasible in the region in question. Degradation of the neutrons from Sb-Be by various scattering processes in any source large enough to be useful poses the main difficulty in determining the neutron energy with greater precision. Several measurements by various methods and with sources of different sizes have been made in the past, with values being quoted from 25 to 35 kilovolts. The present work concerns the possibility of narrowing the limits of error in this energy by a comparison of transmission cross sections using Sb-Be photoneutrons with transmission cross sections measured with the Argonne electrostatic generator in the 20 to 40-kilovolt region.

Reproducible values of the cross section were obtained for five different elements. These lead to values of the energy of the Sb-Be neutrons that range from 22 to 28.5 kev with an average value of 25 kev.

The method used involved a simple determination of total cross section by transmission measurements for each sample. Possible values of the energy are obtained from the intersecting of a horizontal

line at the observed value of the cross section with a curve of cross section vs. energy . The curves used are reproduced in AECU-2040, Compilation of Neutron Cross Sections. The energy determined with any element was considered satisfactory when it could be reproduced within 3% by samples of different thickness. Serious discrepancies in the density and cross section measurements on Fe caused the results on this element to be discarded. Only one sample of cobalt, in powder form, was available, and extra precautions were taken to insure proper measurement of its density. The uncertainty in the value of the density did not seriously affect the value of the energy obtained.

To eliminate complex theoretical considerations of multiple scattering and the scattering-in effect, samples were chosen as thin as possible for high transmission, and each transmission cross section was determined relative to the cross section of carbon. The carbon, in the form of a graphite plug, reproduced the geometry of each sample in transmission and was modeled closely for each sample in over-all dimensions.

To reduce room scattering the source and counter were mounted on opposite ends of a light framework suspended 12 feet high in the center of a large room. Between source and counter was mounted a paraffin collimator consisting of two cylinders, each larger than the sensitive area of the counter, with conical apertures to define the beam. The boron trifluoride pulse ion chamber was surrounded by a paraffin moderator for efficiency, and the whole surrounded by 120 mils of cadmium to remove any neutrons scattered by the collimator.

A series of readings consisted of (1) open beam, (2) carbon plug transmission, (3) sample transmission, and (4) open beam. Any run was discarded if the open beam reading varied more than 2% from beginning to end of the run. Each counting period was long enough to achieve 1% statistics.

The transmissions of the samples were calculated using the following concept:

N_o - count observed with no scatterer in place (open beam)

N_b - latent scattered count, including collimator and room scattering

N_{tb} - true beam ($N_o - N_b$)

N_c - count observed with carbon scatterer in beam (closed beam)

N_s - count observed with sample in beam

T_c - transmission of the carbon plug

T_s - transmission of the sample.

T_b closely approximated T_s in this experiment. To determine the true beam:

$$N_o = N_b + N_{tb}$$

$$N_c = N_b + T_c(N_{tb})$$

$$N_o - N_c = N_{tb}(1 - T_c)$$

(1) $$N_{\text{true beam}} = \frac{N_o - N_c}{(1 - T_c)}$$

Similarly, for sample transmission,

$$N_o - N_s = N_{tb}\,(1 - T_s)$$

so that

(2) $$1 - T_s = \frac{N_o - N_s}{N_{tb}} = \frac{(N_o - N_s)\,(1-T_c)}{N_o - N_c}$$

The carbon plugs did not have precisely the same transmissions as their corresponding metal samples, but the differences were less than 5% in every case, thus making multiple scattering and scattering-in errors negligible. Background in the counter did not affect calculations as long as it remained constant.

The factor $(1 - T_C)$ was calculated from the accepted and checked carbon cross section in the 30-kev region, i.e., 4.55 barns. This cross section is constant throughout the energy region under consideration. Density of the graphite used was carefully measured, and the thickness of each graphite plug machined to 1 mil tolerance. Thus:

(3) $\ln \frac{I}{I_0} = \ln T_C = N \sigma X$

where N is number of atoms per cc, σ is the cross section, and X is the thickness of carbon.

When T_S is obtained from eq. (2) using the observed counting rates, the sample cross section is calculated by solving eq. (3) for σ to yield

(4) σ (barns) $= \frac{\ln T_S}{-N X}$

The choice of elements to be used was determined by the requirement that the cross section be energy dependent to a considerable degree in the region from 20 to 40 kev. At least two elements other than those used fulfilled this condition but were not utilized. The energy vs. cross section curve for aluminum was not well resolved above 24 kev, and cerium was not available in a readily usable form. A more complete supply of samples in better quality would have expedited greater accuracy, though at greater expense. It is proposed by the members of the Van de Graaff group that a further study be made after a re-examination

of the transmission cross sections as a function of energy with improved resolution in energy.

The detailed results are as follows:

Element	Cross Section (barns)	Indicated Energy (kev)	Remarks
V	23.9	23.5	Resonance peak makes 19 kev possible
Ti	34.0	28	26 to 30 kev possible variation
Mn	13.0	24	21 kev possible
Co	16.8	28.5	Possible 5% error in sample density
Ni	20.9	22	30 kev possible

XI. The Average Charge of the Daughter Atoms from the Isomeric Transition of Br^{80m}

(S. Wexler)

The average positive charge of the product atoms after isomeric transition of 4.4-hr Br^{80m} was previously reported to be approximately 10 electron units.[1] The experiment measured the positive ion current produced by the decay of C_2H_5 Br^{80m} at low pressure in a spherical electrode system. The current collected by a probe was compared with the disintegration rate. This report gives results of further observations in which the ion current of the decay products was measured in the large cylinder already described.[1] For these studies the outer shell was made + 1335V and the repeller grid - 90V relative to the probe. The ethyl bromide pressure was approximately 5×10^{-4}mm. Except for these conditions the procedures were those followed in the experiments with the spherical chamber.

The results of four determinations appear in TableVI. The average charge produced by the isomeric decay of Br^{80m} is seen to vary from 10 to 13 positive units, and is to be compared with the variation of 8 to 12 electron units observed with the spherical system. The close agreement suggests that the observed result is not decisively influenced by the geometry of the apparatus used.

It is of interest to compare these findings with available theoretical estimates of the average orbital electron loss in this transition, which is characterized by internal conversion and Auger processes.

---

[1] S. Wexler, ANL-4963, Quarterly Report for March, April and May, 1952.

The average charge on a bromine atom has been calculated by Cooper[2] to be +4.7 e.u. after the electronic re-orientation which follows a vacancy in the K-shell. By combining Cooper's results with the K and L conversion coefficients of the Br^{80m} transitions[3,4] we estimate the positive charge to average 6.3 units after the decay. This figure agrees well with +6.8 electron units deduced earlier from fluorescene yield data,[1] but is about half the experimental finding. Considering the difficulties inherent in the calculation, however, the lack of more perfect agreement is not surprising.

---

[2] E. P. Cooper, Phys. Rev. 61, 1 (1942).

[3] P. Rothwell and D. West, Proc. Phys. Soc. (London) 63 A, 539 (1950).

[4] M. Goldhaber and A. W. Sunyar, Phys. Rev. 83, 906 (1951).

Table VI

Average Charge of Daughter Atoms from Isomeric Transitions of Br^{80m}

Positive Ion Current (amp)	Pos. Charges Collected per Second (electron units)	Dis./Sec of Br^{80m} in Ion Chamber	Ave. Pos. Charge per Disintegration (electron units)
4.6×10^{-14}	3.0×10^{5}	2.3×10^{4}	13
8.0×10^{-14}	5.1×10^{5}	4.9×10^{4}	10
7.8×10^{-14}	5.1×10^{5}	4.8×10^{4} (a)	11
8.7×10^{-14}	5.6×10^{5}	4.5×10^{4} (a)	13

(a) Cu cylinders rather than glass decay flasks were used in the disintegration rate measurements.

XII. Average Electric Charge of K^{41} Atoms Formed by the Beta Decay of A^{41}

(S. Wexler)

The average charge carried by daughter atoms after β^--emission of the individual Kr and Xe nuclides in a mixture of fission-produced noble gases was previously observed to be somewhat greater than one electron unit.[1] The result was definitely higher than the charge of approximately +1.0 e.u. found on the products from beta decay of molecular tritium and of carbon -14 dioxide. This was attributed to the presence among the decay products of a small fraction of highly charged ions formed from partial conversion of γ-rays which follow some of the beta-rays. To avoid this complication, a determination of the average charge of K^{41} daughter atoms from A^{41} decay was made, since this nuclide may be considered a pure beta emitter for the purposes of this experiment.[2]

As in earlier studies, the positive current of the K ions was measured in a large cylinder into which the A^{41} was introduced at low pressure. The observed current was compared with the disintegration rate of the argon activity. The latter was determined by diluting with inert argon an aliquot of the active gas taken at a pressure equal to that in the large chamber, and then pumping the mixture into a small gas cell.[3] The A^{41} was counted under an end window counter from a position of known geometry. Proper corrections were made

---

[1] S. Wexler, ANL-4963, Quarterly Report for March, April and May 1952.

[2] For the decay scheme of A^{41} see G. T. Seaborg and I. Perlman, Rev. Mod. Phys. 20, 585 (1948).

[3] The construction and geometry of the gas cell were identical to the one described by F. D. Rosen and W. Davis, Jr., "Absolute Beta Counting of Radioactive Gases Using End Window Geiger-Muller Counters," Report K-678. The average geometry of this arrangement was determined by these authors to be 0.015.

for absorption and scattering of the betas. The A^{41} activity was produced by pile neutron irradiation of pure argon gas.

Preliminary experiments of the type described[1] demonstrated that essentially all the K^{41} ions were collected by the current-measuring probe when the cylindrical shell was +1335V relative to the probe. A voltage of -90V on the grid surrounding the collector was sufficient to prevent secondaries from leaving its surface. The pressure of the active argon in the chamber varied from 1.5 to 8.0 x 10^{-3}mm. Observed currents decreased to half values in times varying from 100 to 115 minutes, in good agreement with the value of 110 min for the half-life of A^{41} usually given.

Assembled in TableVII are the results of seven measurements. The number of positive charges collected per second (Column 3) is derived directly from the observed current (Column 2) and has been corrected for the 12 per cent closed area of the grid. The average charges per disintegration of A^{41} listed in the final column are seen to vary from 0.8 to 1.1 positive electron unit.

The results indicate that the charge of the potassium daughter atoms from beta decay of A^{41} is approximately one unit. Since the charge may be accounted for entirely by the increase in nuclear charge, these findings imply that orbital electron ionization is not a significant effect in purely beta transitions. The result agrees with previous studies on other beta emitters[1] but is at variance with prediction.[4] Further, the lack of significant electron loss in the beta process suggests that de-excitation of the daughter atom probably occurs by emission of radiation. Recent

---

[4] A. Migdal, J. Phys. (USSR) 4, 449 (1941).

calculations show that about 100 e v of excitation energy resides with the product atom after the beta emission.[5]

---

[5] R. Serber and H. S. Snyder, Phys. Rev. 87, 152 (1952).

Table VII

Average Charge of Potassium Atoms After β^- Decay of A^{41}

Expt.	Positive Ion Current (amp)	Pos. Charges Collected/sec (electron units)	Dis./sec of A^{41} in Ion Collection Chamber	Ave. Pos. Charge/Dis. (electron units)
1	3.2×10^{-14}	2.3×10^5	2.1×10^5	1.1
2	3.8×10^{-14}	2.7×10^5	3.1×10^5	0.9
3	3.5×10^{-14}	2.5×10^5	2.6×10^5	1.0
4	3.4×10^{-14}	2.4×10^5	2.6×10^5	0.9
5	1.5×10^{-14}	1.0×10^5	9.6×10^4	1.1
6	3.6×10^{-14}	2.5×10^5	3.1×10^5	0.8
7	2.4×10^{-14}	1.7×10^5	1.6×10^5	1.1

XIII. Half-Lives of Eu^{152}, Eu^{154} and Sm^{151}

(D. G. Karraker, R. J. Hayden and M. G. Inghram)

The half-lives of Eu^{152}, Eu^{154} and Sm^{151} have been measured directly by mass spectrometric methods. In each case, the half-life was determined by the change with time of the isotopic constitution of samples containing an appreciable percentage of the nuclide under investigation. For Eu^{152} and Eu^{154} the sample used for the determination of the half-lives was a normal europium sample irradiated in a pile. Data on this sample have been used previously for an indirect determination of the half-lives of Eu^{152} and Eu^{154}. [1]

The half-life of Sm^{151} was determined by the change in isotopic abundance of Sm^{151} in a sample of purified fission-produced samarium, used for a previous indirect determination of the half-life by Inghram, Hayden, and Hess. [2]

In every case, isotopic analysis was made on a 12 inch radius of curvature 60° deflection mass spectrometer. [3] The europium sample was purified from its daughters by elution with pH 3.06 ammonium citrate from an ion exchange column filled with Dowex 50 resin. No further purification was made on the samarium. The data pertinent to the calculations and the results are given in Table VIII.

---

[1] R. J. Hayden, J. H. Reynolds, and M. G. Inghram, Phys. Rev. 75, 1500 (1949).

[2] M. G. Inghram, R. J. Hayden, and D. C. Hess, Phys. Rev. 79, 271 (1950).

[3] M. G. Inghram, D. C. Hess, and R. J. Hayden (to be published).

Table VIII

	Time for Decay (yrs.)	% Decay	Half-life (yrs.)
Eu^{152}	3.4	16.7 ± 2.4	13 ± 2
Eu^{154}	3.4	13.9 ± 3.3	16 ± 4
Sm^{151}	3.8	3.6 ± 0.9	73^{+25}_{-14}

The errors quoted for the half-lives consider only the mean deviation of the isotopic determinations.

The value for the half-life of Sm^{151} is in fair agreement with the 122-year value determined indirectly by Inghram, Hayden, and Hess, but disagrees markedly with the 10^3-year half-life obtained by Marinsky.[4]

The serious discrepancy between the half-lives determined for Eu^{152} and Eu^{154} and the half-lives obtained by Hayden, Reynolds, and Inghram may be caused by an experimental error in the determination of the absolute amount of the gadolinium present after bombardment. The presence of a short-lived isomer of Eu^{154} would otherwise be necessary to explain the error in half-life of Eu^{154}. No such isomer is known.

The values for the branching ratios of the 9.2-hour Eu^{152}, the 13-year Eu^{152}, and the proportion of Eu^{151} capture that goes to each of the two Eu^{152} isomers, all measured indirectly by Hayden, Reynolds, and Inghram, are almost certainly in error since they involve the above determined half-lives. No statement about the correct values can be made without a repetition of their experiment.

---

4 Way, Fano, Scott, and Thew, Nuclear Data, National Bureau of Standards, Circular 499 (1950).

XIV. An Investigation of the Heat of Vaporization of Carbon (William A. Chupka and Mark G. Inghram)

There is considerable controversy over the value of the heat of vaporization of carbon. Three possible spectroscopic values for the dissociation energy of CO coupled with well established thermodynamic data give three possible values for this quantity. The three values are 136 kcal/mole, 141 kcal/mole, and 170 kcal/mole. The controversy revolves around two questions; the accommodation coefficient for evaporation, and the identity and relative amounts of the evaporating species. An accommodation coefficient near unity, assuming that the evaporation occurs largely as C, would favor the highest value, according to available data on the rate of evaporation from a graphite surface. Doehaerd, Goldfinger, and Waelbroeck[1] claim that the accommodation coefficient is actually about 0.001. If this is true, one of the lower heats of evaporation is correct. Waelbroeck claims that the major part of the evaporating species is C_2. This is in contrast with Brewer's determination[2] where he finds the C_2 evaporation to be of the order of 0.0001 of the total evaporation. The main objection of Brewer to the experiments of Doehaerd, et al. is the possibility of insufficient outgassing of their graphite sample.

One possible method of resolving these difficulties is to use a mass spectrometer to identify and measure the relative amounts of the various species evaporated from a graphite surface as a function of surface temperature. We have made preliminary measurements using this technique.

---

[1] Th. Doehaerd, P. Goldfinger, and F. Waelbroeck, J. Chem. Phys. 20, 757 (1952).

[2] L. Brewer, Gilles, Jenkins, J. Chem. Phys. 16, 797, (1948).

The technique used consisted of bombarding the constituents evaporated from a carbon filament with electrons of controlled energy and determining the mass of the ion produced with a standard single focussing magnetic analyzer. The constituents were thus identified both by mass and by appearance potential. The C+ ion appeared at an electron bombarding energy of 11.1 volts, the C_2+ appeared at approximately 12 volts. The 11.1 volt appearance potential for C+ ion indicates that the evaporation of C occurs in the ground state. This assumes that the half-life of the excited 5S state is longer than the transit time between evaporation and ionization. The time of transit is about 10^{-5} sec.

In addition to mass resolution and appearance potentials the ion beams were studied by retarding potential techniques. This served to show whether the evaporating species have kinetic energy in excess of thermal energies. According to a theory of Herzberg[3] carbon atoms may evaporate over a potential barrier which would give resulting atoms an excess kinetic energy in an amount equal to the difference between the heat of sublimation and the activation energy. Any excess kinetic energy would have to be subtracted from the apparent heat of vaporization obtained by temperature plots of evaporation from a surface in order to get the true heat of sublimation.

The variation of the evaporation of carbon atoms with temperature is shown in Fig. 3. The slope indicates an activation energy for evaporation at the specified temperature of approximately 176 ± 10 kcal/mole.

---

[3] Herzberg, Chem. Rev. 20, 145 (1937)

FIGURE 3.

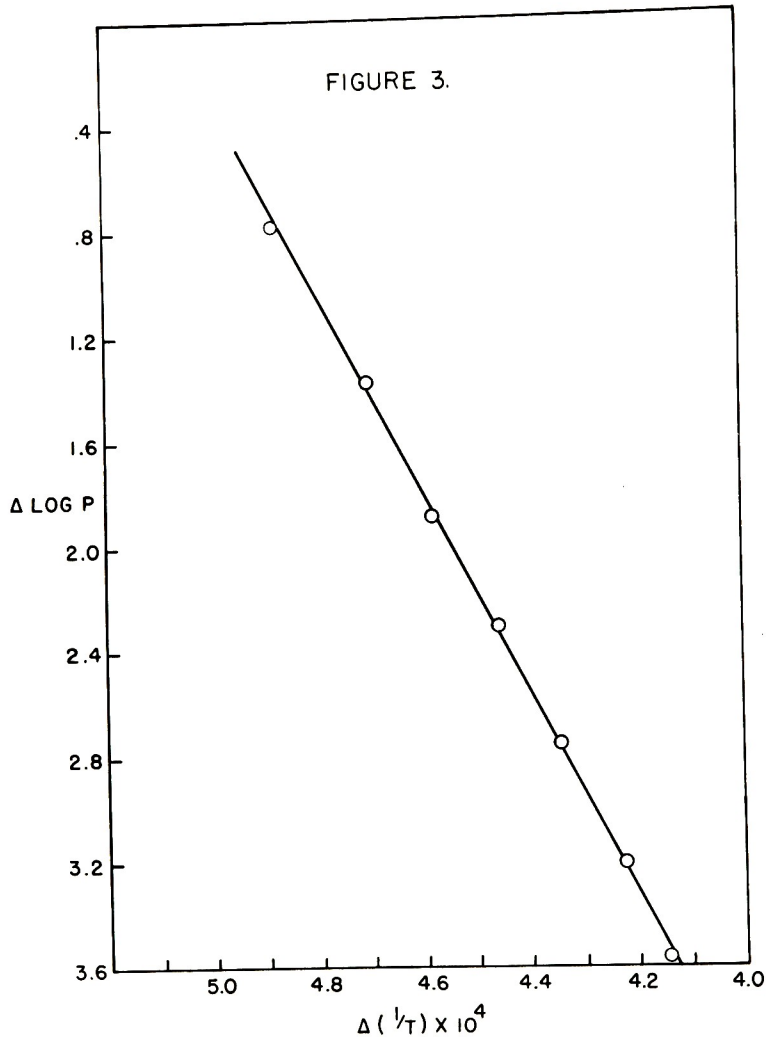

This gives a $\Delta H(0°K)$ of 171 ± 10 kcal/mole. The close agreement with the high spectroscopic value is clearly fortuitous, but the lower spectroscopic value is not acceptable as an activation energy.

Measurements of the energy of the C+ ions showed them to have thermal energies within ± .3 volt. This value is incompatible with Herzberg's suggestion of a potential barrier of the order of 1.5 volts. On the other hand, the proposal of Herzberg, Herzfeld, and Teller[4] is not affected by this observation so that a low accommodation coefficient is still possible.

The ratio of C/C_2, assuming equal ionization cross sections, was found to be 1.2 at 2300° K. This ratio decreases with an increase in temperature, but accurate measurements have not yet been carried out because of interference of a strong Na+ ion beam. There still remains a slight possibility that the C_2+ is formed from the free radical C_2H since the corresponding appearance potential is not known. The ratio C_2/C_2H, assuming equal ionization cross sections, was approximately unity.

It was found that the intensity of hydrocarbons and free radicals went up with temperature. The ratio of carbon to total evaporation did improve throughout the course of an experiment. This indicates that spurious results might be obtained under conditions of insufficient outgassing and where mass resolution is not used.

Further experiments are planned to extend further the temperature range of the experiment and to investigate more completely the accommodation coefficient.

---

4 Herzberg, Herzfeld, and Teller, J. Phys. Chem. 41, 325 (1937).

XV. The Electron Affinity of Carbon

(William A. Chupka and Mark G. Inghram)

The negative ion emission from a heated carbon filament was investigated with a mass spectrometer in an attempt to measure the electron affinity of the carbon atom. Less than 5% of the observed negative ion emission was C^-, and much of the C^- emission appeared to be due to sources other than thermal ionization on the carbon surface. These observations indicate that the published values for the electron affinity which were obtained without mass identification are somewhat too high.

XVI. Crystallographic Studies
(H. A. Plettinger and W. H. Zachariasen)

1. The Crystal Structure of Metaboric Acid, HBO_2

A preliminary account of this investigation was reported last year in ANL-4659, p. 65. Since then a second approximation in the refinement of the 27 parameters for boron and oxygen atoms has been carried out. The third and final approximation is expected to yield also the positions of the hydrogen atoms. The third approximation involves the evaluation of a 3-dimensional Fourier series with 900 terms. The computations will be carried out on the XRAC analog computer at Pennsylvania State College in the near future.

2. The Crystal Structure of Orthoboric Acid, H_3BO_3

A precision determination of the structure of orthoboric acid is under way. The experimental part of the investigation has been completed.

XVII. The Remarkable Longevity of C^{14} and the Structure of Light Nuclei

(D. R. Inglis)

The long life of C^{14} (5,400 years, E_{max} = 155 kev) stands in puzzling contrast with the short life of He^6 (0.84 sec, E_{max} = 3.35 Mev) and other light nuclei, and the somewhat implausible special assumptions that have been introduced to account for it[1,2] have been disproved by subsequent experimental findings.[3,4] According to the usual beta-decay theory with a Gamow-Teller term in the interaction and with the two nuclear matrix elements assumed about equal, the life of C^{14} is too long by a factor 10^6.

Whereas nuclei considerably heavier than oxygen seem to have many of their features accounted for by the (jj) coupling of the well-known Mayer-Jensen shell model, the nuclei from beryllium to oxygen have level sequences that seem to correspond most closely to intermediate coupling.[5] In intermediate coupling, the ground state of the final nucleus N_{14} (two nucleons missing from the p-shell, configuration p^{-2}) is almost 90% of ^3D and only about 10% of ^1P and ^3S together. The ground state of C^{14} consists only of S and P components, without any D,

---

1 E. Feenberg and K. C. Hammack, Phys. Rev. 75, 1877 (1949), quoting also H. Primakoff.

2 E. Gerjuoy, Phys. Rev. 81, 62 (1951).

3 A pure ^3D ground state of N^{14} is inconsistent with the failure of the energy level sequence to resemble Russell-Saunders coupling, which would require two very low excited states (^3D with T = 0) not found by Van de Graaff, Sperduto, Buechner and Enge, Phys. Rev. 86, 966 (1952). The isobaric spin selection rule forbids the O^{16} (d, γ) N^{14} transition to the (J, T) = (0, 1) state, which is indeed unobserved, but not to these (2, 0) and (3, 0) states.

4 D. A. Bromley and L. M. Goldman, Phys. Rev. 86, 790 (1952).

5 D. R. Inglis, Phys. Rev. 87, 915 (1952). The intermediate coupling interpretation of the other elements of the p-shell is developed in a subsequent paper to appear in the Reviews of Modern Physics for April, 1953.

and the L-selection rule means that there are only S and P contributions to the beta-decay matrix element going to the small components of the final state. Thus the 10% gives a factor 10^2 in the lifetime, inadequate but in the right direction. Unfortunately, the S and P contributions to the matrix element are found to have the same sign, and cannot fortuitously cancel one another. If the missing factor 10^{-2} in the matrix element is to be attributed to fortuitous cancellation, as appears to be the only remaining possibility, it must arise from an admixture of excited configurations into the wave function of the final state to the extent of at least about 10%. This rather small amount of configuration interaction is quite compatible with the validity of the central model with unmixed configurations as a reasonable approximation for most qualitative features of nuclear structure.

XVIII. States of Light Nuclei from the jj-coupling Model
(Dieter Kurath)

A paper having this title has appeared in the Physical Review, 88, 804 (1952). The following is the abstract of its content.

The ordering of energy levels is presented for 1 p shell nuclei in the jj-coupling model. Comparisons of the jj and LS model predictions with experiment are given for angular momenta and magnetic moments of the ground states as well as for the shape of the binding energy curve. No decisive favoring of either model is evident.

XIX. The Neutron Capture Cross Section of Fe^{56}

(J. E. Monahan)

If the capture cross section of iron could be determined with any accuracy, it should be possible to make some predictions about structural effects in a fast pile. The energy dependence of the (n, γ) cross section for an isotope can be obtained on the basis of the statistical model of nuclear reactions.[1] The resulting equations contain one arbitrary parameter which must be determined experimentally. Unfortunately the existing data for Fe^{56}, the most abundant isotope of iron (92%), are doubtful. There are, however, several interesting features of the capture cross section of this isotope which seem less uncertain. These are discussed below.

The cross section for (n, γ) processes may be written

$$\sigma(n,\gamma) = \sum_{l,j} \sigma_l^{(j)}(n) \frac{\Gamma_\gamma^{(j)}}{\Gamma^{(j)}}$$

where $\sigma_l^{(j)}(n)$ is the cross section for formation of a compound nucleus of spin j by incident neutrons of angular momentum l. $\Gamma_\gamma^{(j)}$ and $\Gamma^{(j)}$ are the radiation and total widths of the state j evaluated at the appropriate excitation energy. In the energy range considered below the probability of emission of charged particles is negligible so that the total width may be taken as the sum of the width for neutron emission and the radiation width. All quantities with the exception of $\Gamma_\gamma^{(j)}$ are well known. Margolis[2] has obtained an estimate of the energy dependence of $\Gamma_\gamma^{(j)}$; his calculations involve one arbitrary parameter, namely

---

1 H. Feshbach and V. Weisskopf, Phys. Rev. 76, 1550 (1949).

2 B. Margolis, Phys. Rev. 88, 327 (1952).

$D^{(j)}(B)/\Gamma_r^{(j)}(B)$, where $D^{(j)}(B)$ is the spacing of levels of the same spin and parity in the compound nucleus evaluated at the binding energy of the captured neutron, B. This ratio can be shown to be independent of j by assuming that the energy dependence of the compound nuclear level density is that obtained by treating the nucleus as a degenerate gas.

The most probable level scheme of Fe^{56} consists of a ground level of spin zero with a first excited state of spin and parity 2+ at 0.845 Mev. The (n, γ) cross section, based on these assumptions, is given in the following table for four values of the ratio $D^{(j)}(B)/\Gamma_r^{(j)}(B)$:

	$\sigma(n,\gamma)$ (milli barns)			
E (Mev)	$D^{(j)}/\Gamma_n^{(j)} = 360$	= 720	= 2260	= 4520
47	137.54	76.93	28.52	15.91
144	73.42	42.84	18.22	9.56
384	56.33	31.52	11.71	6.53
422	55.68	31.26	11.86	6.64
769	55.44	31.18	11.61	6.70
845	55.45	31.20	11.60	6.89
892	33.96	18.37	6.09	3.35
989	33.67	17.24	5.73	2.93
1229	25.31	12.88	4.16	2.10
1614	27.18	13.86	4.44	2.24
2074	34.09	17.36	5.61	2.81
2459	46.40	23.76	7.71	3.88

In the above table E is the energy of the incident neutrons. For these calculations B was taken to be 8 Mev, and it is assumed that no level exists for $0.845 \text{ Mev} < E < 2.500 \text{ Mev}$.

Hughes et al.[3] have found a smooth dependence of measured isotopic activation cross sections on atomic weight A for $A < 100$. If such a dependence exists, the capture cross section for an element with no

[3] D. Hughes, W. Spatz, and N. Goldstein, Phys. Rev. 75, 1781 (1949).

measurable activation could be predicted. For Fe^{56} a cross section of 6.5 milli-barns at 1 Mev is indicated. On the basis of the above calculations this would mean that

$$\frac{D^{(j)}(B)}{\Gamma_r^{(j)}(B)} \simeq 2000.$$

Assuming a level width of $\sim$1000 ev, the radiation width evaluated at B is $\sim$0.5 ev, a value which is plausible for nuclei in the neighborhood of A = 56.

Two features of these cross sections are relatively independent of the assumed value of $D(j)/\Gamma_r(j)$. First $\sigma(n, \gamma)$ is essentially constant for energies greater than $\sim$0.20 Mev and less than the energy of the first excited level. This is probably a consequence of the assumption of zero spin for the ground level of the target. Secondly the shape of the curve σ vs. E is independent of this ratio, at least to a first approximation.

XX. The Effective Length of an Electrostatic Analyzer
(J. E. Monahan)

A paper on this subject has been submitted for publication to the Journal of Applied Physics.

The general formula for the effective length of an electrostatic analyzer with rounded corners is derived using a modified Schwartz transformation. It is found that for a proposed practical analyzer the rounding of the corners introduces a correction of about 0.1 percent in the effective length of the analyzer.

XXI. Applications of the Mauro Picone Theorem for Heat Conduction (George W. Evans II)

A paper on this subject has been put out as AECU-2252, UAC-647. The following is an abstract of its contents.

Use is made of a restricted statement of a theorem due to M. Picone (Math. Ann., 101, 701-712 (1929)), which essentially asserts that a non-constant solution of the heat conduction equation must have its maximum and minimum values along the boundary of the half-open xt-region of description, to prove the uniqueness of the solution $u(x,t)$ of the differential equation

$$a u_{xx} = u_t - Q(t) \qquad \text{for } 0 \leq x < a$$

and the differential equation

$$a u_{xx} = u_t \qquad \text{for } a < x \leq L$$

for the initial condition

$$u(x,0) = f(x)$$

and the boundary conditions

$$u_x(0,t) = 0,$$

$$u_x(a+,t) = u_x(a-,t) = u_x(a,t),$$

$$u(a+,t) = u(a-,t) = u(a,t),$$

and

$$k\, u_x(L,t) = h(t)\, \left[u(L,t) - g(t) \right],$$

where $Q(t)$, $h(t)$, and $g(t)$ are known functions. The Picone theorem is also used to analyze the action of a thermal controlling unit, which consists of two thermocouples, for an oven.